1. Introduction

These lectures provide a basic introduction to infrared (IR) astronomy. Key references are provided to allow the reader to pursue subjects in greater detail. This work does not attempt to cover all aspects of IR astronomy; it focuses on basic background information, observing techniques, photometry, absolute calibration, and some aspects of instrumentation.

The foundation for the IR detectors used today was established in the1960s and 1970s, and this led to the growth of ground-based IR astronomy as a mature field. Efforts to get above the atmosphere with suborbital rockets started about 1965, and these led to a series of increasingly sophisticated space-based observatories.

See Price (2009) and Rieke (2009) for detailed historical accounts.

Notes:
Price, S. D. (2009). "Infrared Sky Surveys." Space Science Reviews **142**: 233-321.
Rieke, G. H. (2009). "History of infrared telescopes and astronomy." Experimental Astronomy **25**: 125-141.

The period of 1960 to 1975 was one of great advances in infrared astronomy. Pioneered primarily by physicists the field gradually grew into an important astronomical discipline. A nice summary of these early years is given by Low, Rieke, and Gehrz (2007).

During these years the major advances in detectors was the development of the gallium-doped germanium bolometer in 1961 by F. Low and the development of the InSb detector by D. Hall and collaborators in 1975. These detectors were much more sensitive than previous detectors and helped to greatly accelerate the development of infrared astronomy.

These early detectors consisted of a single element and special techniques were developed to overcome the background and to do sky maps. Some of the advances in the early years included:

1960-1970: development of the gallium-doped germanium bolometer, start of IR airborne astronomy, IR balloon observations, IR observations with sounding rockets; completion of the Two Micron Survey by Neugebauer and Leighton (this was the first IR sky survey). Initial observations of the solar system, evolved stars, star forming regions, the galactic center, and galaxies were made.

Notes:

Low, F. J., G. H. Rieke and R. D. Gehrz (2007). "The Beginning of Modern Infrared Astronomy." Annual Review of Astronomy and Astrophysics **45**: 43-75.

1970-1975: first IR sky survey above the atmosphere using sounding rockets; initial IR observations in the southern hemisphere, development of the InSb discrete detector (arrays of InSb detectors started to become available around 1984). The basic elements of an IR-optimized telescope were developed: sky chopping, telescope nodding, undersized secondary, up-looking instruments (to minimize emissivity).

1975-1980: the largest IR telescopes in the world at the time were built on Mauna Kea (the United Kingdom Infrared Telescope (UKIRT) and the NASA Infrared Telescope Facility (IRTF). All large telescope were subsequently designed as optical/infrared telescopes with the Gemini telescopes specifically designed to be IR-optimized.

Notes:

List of selected IR optimized and optical/IR facilities

1979 UKIRT (3.8m) and NASA IRTF (3.0m); IR optimized
1993/1996 Keck I and Keck II (2 x 10.0m)
1998-2000 Very Large Telescope (VLT; 4 x 8.2m)
1999-2000 Gemini North and South (2 x 8.1m); IR optimized
1999 Subaru (8.2m)
2005-2008 Large Binocular Telescope (LBT; 2 x 8.4m)

~2019 Tokyo Atacama Observatory (TAO; 6.5m)
~2025 Extremely Large Telescope (ELT; 39.5m)
~2025 Thirty Meter Telescope (TMT; 30.0m)
~2025 Giant Magellan Telescope (GMT; 21.7m equivalent)

Notes:

We live in a special time of great increases in telescope capability.

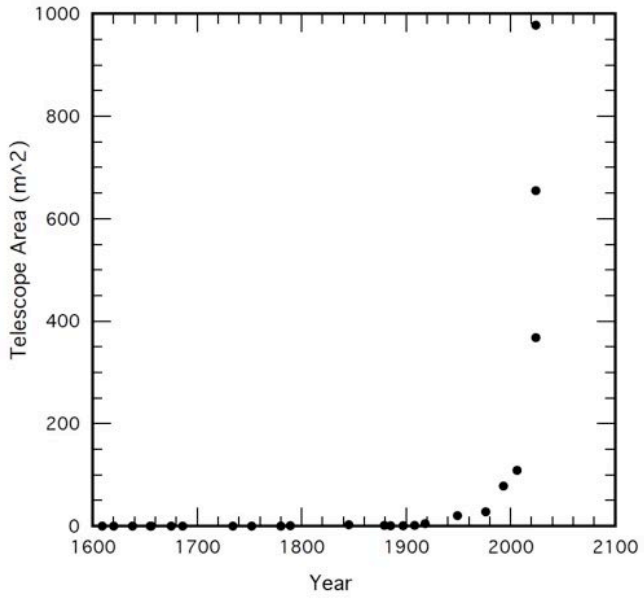

Notes:

Here is another way to look at the growth of telescope collecting area.

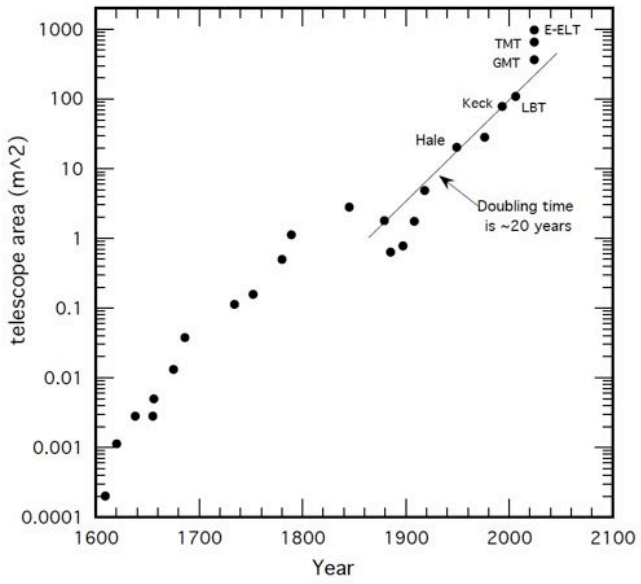

Notes:

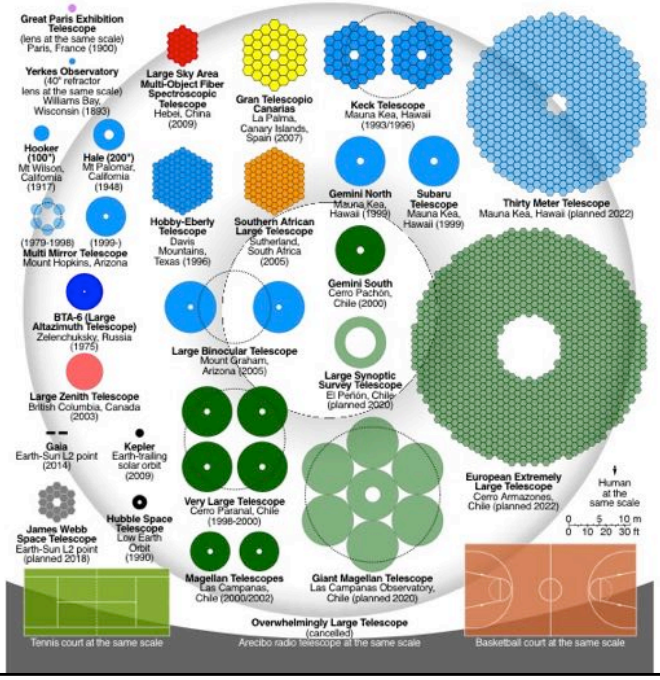

Another way to view growth in telescope collecting area:

Graphical comparison of telescope apertures.

Notes:
https://en.wikipedia.org/wiki/List_of_largest_optical_reflecting_telescopes

In addition, there were many space observatories launched starting with the Infrared Astronomy Satellite (IRAS) which surveyed the sky in 1983. This was the first IR sky survey from space and it made fundamental discoveries in the solar system, the Milky Way galaxy, and external galaxies.

List of IR space observatories:

1983 Infrared Astronomy Satellite (IRAS; 0.57m)
1989 Cosmic Background Explorer (COBE; 0.19m)
1995 Infrared Space Observatory (ISO; 0.60m)
1995 Infrared Telescope in Space (IRTS; 0.15m)
1996 Midcourse Space Experiment (MSX; 0.35m)
1998 Submillimeter Wave Astronomy Telescope (SWAS; 0.55m x 0.71m)
2001 Wilkinson Microwave Anisotropy Probe (WMAP; 1.4m x 1.6m)
2003 Spitzer Space Telescope (SST; 0.85m)
2006 Akari (0.67m)
2009 Wide-field Infrared Survey Explorer (WISE; 0.40m)
2009 Herschel Space Observatory (3.5m)
2009 Planck (1.9m x 1.5m)

2019 James Webb Space Telescope (JWST; 6 m)

Notes:
The Hubble Space Telescope, launched in 1990, was not designed as an IR telescope but it had near-IR instruments.

Some of these observatories will be discussed in detail later.

1.1 Some science highlights in IR astronomy

The all-sky images shown here were made at optical wavelengths (Mellinger 2009) and by the 2MASS near-IR sky survey.

The much lower extinction at near-IR wavelengths is evident. The Galactic Center and disk of the Milky Way is clearly revealed.

This pair of images demonstrates why studies in regions of high interstellar extinction depends on IR observations.

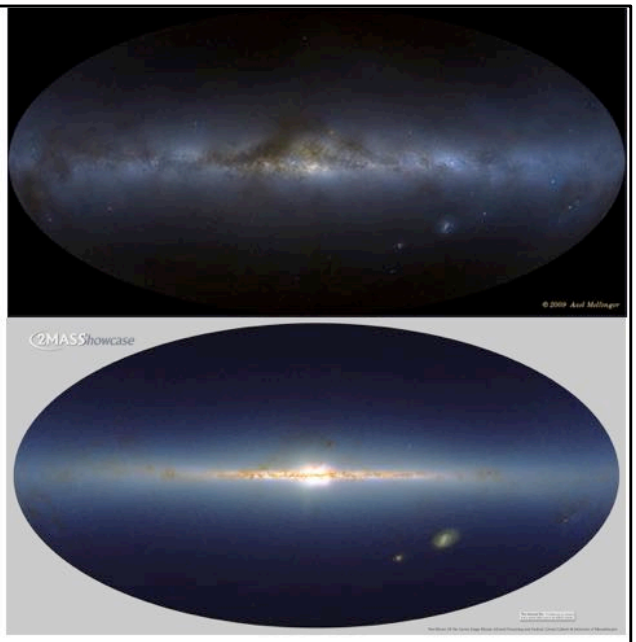

Notes:
2MASS image: https://www.ipac.caltech.edu/2mass/gallery/showcase/allsky_stars/index.html
Visible all sky image: Mellinger, A. (2009). "A Color All-Sky Panorama Image of the Milky Way." Publications of the Astronomical Society of the Pacific **121**: 1180-1187.

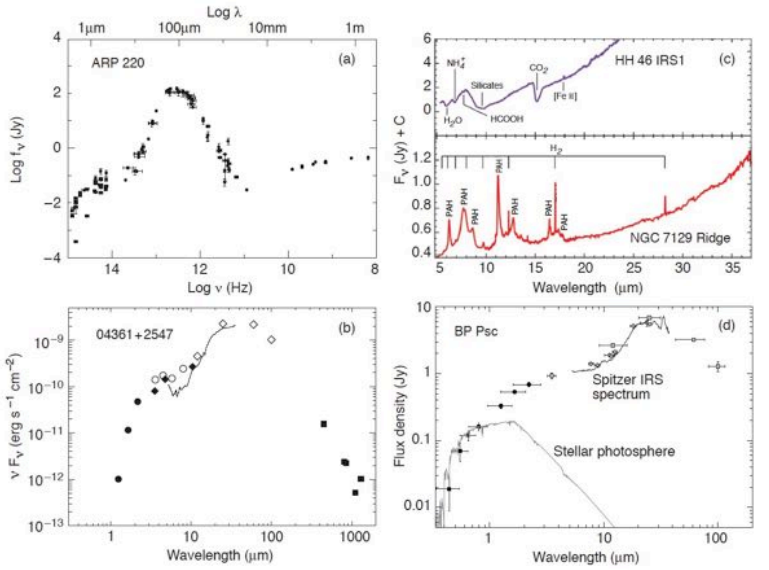

Examples of spectra and spectral energy distributions in the infrared.

(a) Ultraluminous IR galaxy Arp 220. Data from the NASA/IPAC Extragalactic Database (NED).
(b) Class I young stellar object (Furlan et al., 2008).
(c) Ice absorption bands and polycyclic aromatic hydrocarbon emission bands in star-forming regions (from Werner et al., 2006; see also van Dishoeck, 2004 and Peeters, 2011).
(d) Star with a cool dust envelope (Melis et al., 2010).

Notes: Many astronomical sources emit most of their luminosity in the infrared. The entire wavelength range of 1–1000 μm has been accessible in the past few decades with ground-based and space-based observatories. Note the range in flux density of nearly 10^5 and the spectral range of 10^4 in the examples shown.
The IR spectral range is important because many molecules, dust grains, and ice grains in the interstellar medium and circumstellar disks can only be observed in the infrared. The infrared is indispensable for the study of the composition of the interstellar medium, as well as comets, planetary atmospheres, and cool stellar atmospheres, due to the strong molecular bands at IR wavelengths.

Furlan, E. et al. (2008). "Spitzer IRS Spectra and Envelope Models of Class I Protostars in Taurus." The Astrophysical Journal Supplement Series **176**: 184-215.
Werner, M. et al. (2006). "First Fruits of the Spitzer Space Telescope: Galactic and Solar System Studies." Annual Review Astronomy and Astrophysics **44**: 269-321.
van Dishoeck, E. F. (2004). "ISO Spectroscopy of Gas and Dust: From Molecular Clouds to Protoplanetary Disks." Annual Review of Astronomy and Astrophysics **42**: 119-167.
Peeters, E. (2011). The PAH Hypothesis after 25 Years. Proc. IAU Symposium 280. **7:** 149-161.
Melis, C. et al. (2010). "Shocks and a Giant Planet in the Disk Orbiting BP Piscium?" The Astrophysical Journal **724**: 470-479.

In addition to compositional information, the abundance and distribution of interstellar dust can be studied only in the far infrared as shown in this figure (Molinari et al., 2011).

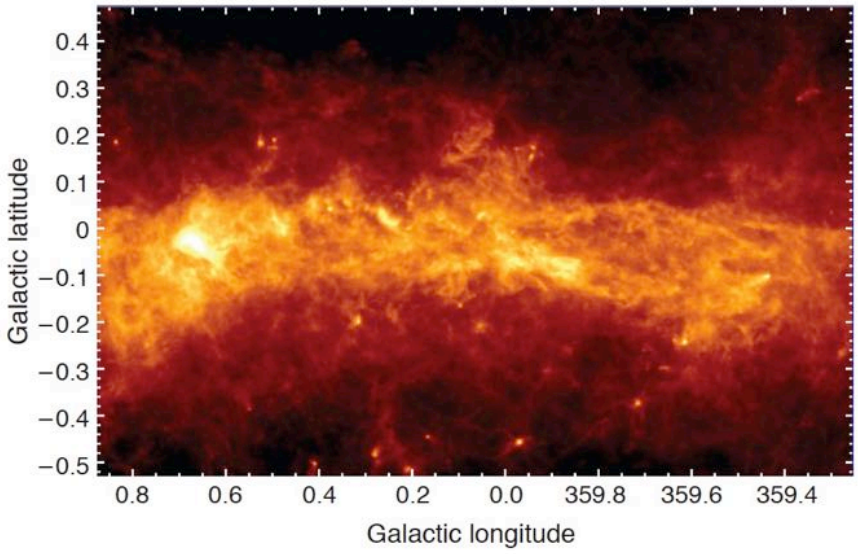

Notes:

Molinari, S. et al. (2011). "A 100 pc Elliptical and Twisted Ring of Cold and Dense Molecular Clouds Revealed by Herschel Around the Galactic Center." The Astrophysical Journal Letters **735**: L33.

Illustration of advances in adaptive optics.

Upper two panels: Images of 51 Eri b taken with at two wavelengths (K1 1.9-2.2 mic, K2 2.1-2.4 mic) with the Gemini Planet Imager adaptive optics instrument on the Gemini South telescope. Lower two panels: Images at Lp (3.8 mic) and Ms (4.7 mic) taken with the NIRC2 AO camera on the Keck telescope.

These images and the spectra obtained by the Gemini Planet Imager show that 51 Eri b has a mass of 2-10 Jupiter masses, a temperature of about 670 K, and a partly cloudy atmosphere.

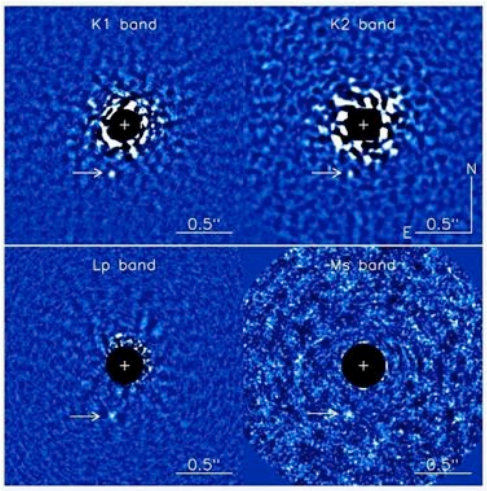

Rajan et al. 2017.

Notes: Adaptive optics in astronomy is typically done in the near-IR since the wave-front correction is at infrared wavelengths and the wave-front distortion measurements are made at the shorter wavelengths.

Rajan, A. et al. (2017). "Characterizing 51 Eri b from 1 to 5 μm: A Partly Cloudy Exoplanet." The Astronomical Journal **154**.

The orbits of stars within the central 1.0" x 1.0" of our Galaxy obtained with the Keck Observatory AO system. The central portion of a diffraction-limited near-IR image of the Galactic Center is displayed. The motions of eight stars are shown. The annual average positions for these stars are plotted as colored dots. Also plotted are the best fitting simultaneous orbital solutions. These orbits provide evidence for a black hole at the center of the Galaxy with a mass of $4 \times 10^6 M_{sun}$. Star S0-102 has a period of only 11.5 years. Ghez et al. 2018.

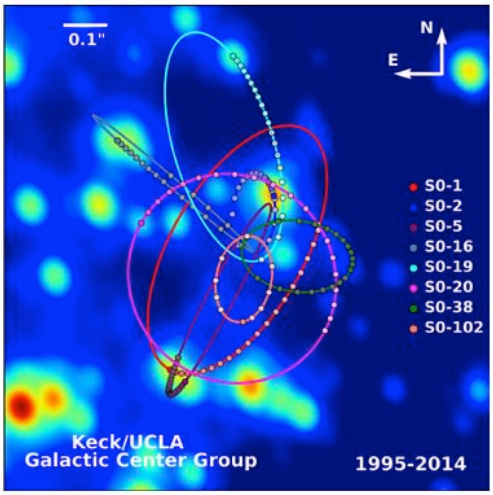

Notes:
Andrea Ghez, UCLA Galactic Center Group, 2018, http://www.galacticcenter.astro.ucla.edu/blackhole.html

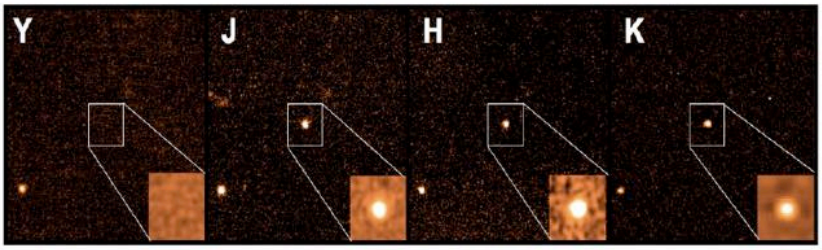

Multiband images at Y (1.02 μm), J (1.26 μm), H (1.65 μm), and K (2.15 μm) of the afterglow of gamma-ray burster GRB 090423 obtained with the UKIRT Wide Field Camera and the Gemini-North Near Infrared Imager. The images shown are approximately 40 arcsec on a side, with North up and East left. The lack of a *Y*-band image implies a redshift greater than 7.8. A spectrum obtained by the Very Large Telescope a (VLT) shows the Lyman-alpha break and a redshift determination of 8.26. From Tanvir et al. (2009).

Notes:
Tanvir, N. R. et al. (2009). "A γ-ray burst at a redshift of z~8.2." Nature **461**: 1254-1257.

1.2 Terminology and units

The following definitions are used for convenience: near infrared (1–5 μm), mid infrared (5–25 μm), far infrared (25–200 μm), and submillimeter (submm) (200–1000 μm). Broadband measurement of radiation from celestial sources are referred to as "photometry," although the term "radiometry" is technically the proper term in fields other than astronomy.

Because terminology for units is sometimes confused, they are summarized in table below.

Units	Radiometric name	Astronomical name
W	flux	luminosity
$W\ m^{-2}$	irradiance; radiant exitance	flux
$W\ sr^{-1}$	intensity	---
$W\ m^{-2}\ sr^{-1}$	radiance	intensity
$W\ m^{-2}\ \mu m^{-1}$; $W\ m^{-2}\ Hz^{-1}$	spectral irradiance	flux density
$W\ m^{-2}\ \mu m^{-1}\ sr^{-1}$; $W\ m^{-2}\ Hz^{-1}\ sr^{-1}$	spectral radiance	surface brightness; specific intensity
$10^{-26}\ W\ m^{-2}\ Hz^{-1}$	---	Jansky (Jy)

From Tokunaga (2000); see also Rieke (2003).

Notes: Although physical units shown in in the table are used for comparison to models, astronomers often use magnitudes. The conversion from magnitudes to physical units is discussed later.

Tokunaga, A. T. (2000). Infrared Astronomy. Allen's Astrophysical Quantities, 4th edition. A. N. Cox. New York, Springer-Verlag: 143.
Rieke, G. H. (2003). Detection of Light: From the Ultraviolet to the Submillimeter. Cambridge, Cambridge University Press.

It is best to plot in consistent units and use SI units. The figure on slide 1-10 shows typical ways that data are plotted.

Figure (a) shows a log-log plot with units of Jy on the y-axis and frequency on the x-axis. This is proper.

Figure (b) is also correct, since $\nu F_\nu = \lambda F_\lambda$ and the flux (W m^{-2}) is plotted on the y-axis.

Figures (c) and (d) show inconsistent units on the y-axis and x-axis. Although it is common to see such mixed units in the literature, it should be avoided. To use Jy on the y-axis and to show a wavelength scale, follow the example of Figure (a).

Proper comparison to physical models requires consistent units. See Soffer & Lynch (1999) for a discussion of how the choice of units affects our interpretation and perception of data.

Notes:
Soffer, B. H. and D. K. Lynch (1999). "Some paradoxes, errors, and resolutions concerning the spectral optimization of human vision." American Journal of Physics **67**: 946-953. This paper can be downloaded at:

https://www.dropbox.com/s/0d5iqjaecpmp36l/Soffer99amJPhys67.pdf?dl=0

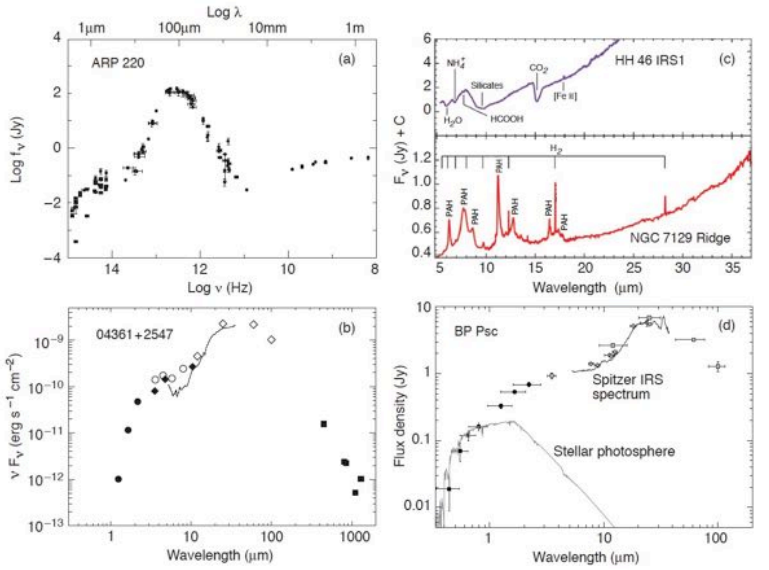

Examples of spectra and spectral energy distributions in the infrared.

(a) Ultraluminous IR galaxy Arp 220. Data from the NASA/IPAC Extragalactic Database (NED).
(b) Class I young stellar object (Furlan et al., 2008).
(c) Ice absorption bands and polycyclic aromatic hydrocarbon emission bands in star-forming regions (from Werner et al., 2006; see also van Dishoeck, 2004 and Peeters, 2011).
(d) Star with a cool dust envelope (Melis et al., 2010).

Notes: Many astronomical sources emit most of their luminosity in the infrared. The entire wavelength range of 1–1000 μm has been accessible in the past few decades with ground-based and space-based observatories. Note the range in flux density of nearly 10^5 and the spectral range of 10^4 in the examples shown.
The IR spectral range is important because many molecules, dust grains, and ice grains in the interstellar medium and circumstellar disks can only be observed in the infrared. The infrared is indispensable for the study of the composition of the interstellar medium, as well as comets, planetary atmospheres, and cool stellar atmospheres, due to the strong molecular bands at IR wavelengths.

Furlan, E. et al. (2008). "Spitzer IRS Spectra and Envelope Models of Class I Protostars in Taurus." The Astrophysical Journal Supplement Series **176**: 184-215.
Werner, M. et al. (2006). "First Fruits of the Spitzer Space Telescope: Galactic and Solar System Studies." Annual Review Astronomy and Astrophysics **44**: 269-321.
van Dishoeck, E. F. (2004). "ISO Spectroscopy of Gas and Dust: From Molecular Clouds to Protoplanetary Disks." Annual Review of Astronomy and Astrophysics **42**: 119-167.
Peeters, E. (2011). The PAH Hypothesis after 25 Years. Proc. IAU Symposium 280. **7:** 149-161.
Melis, C. et al. (2010). "Shocks and a Giant Planet in the Disk Orbiting BP Piscium?" The Astrophysical Journal **724**: 470-479.

1.3 Blackbody radiation and emissivity

Every object in the universe emits thermal radiation. For a perfect blackbody, the emissivity (e) = 1.0, and the spectral radiance is given by the Planck function:

$$B_\lambda(T) = 2hc^2\lambda^{-5}/(e^{hc/k\lambda T} - 1)$$
$$= 1.1910 \times 10^8 \lambda_{\mu m}^{-5}/(e^{14387.7/\lambda_{\mu m}T} - 1) \quad W\,m^{-2}\mu m^{-1}sr^{-1}$$

where $\lambda_{\mu m}$ is the wavelength in micrometers.

In frequency units (ν in Hz),

$$B_\nu(T) = 2h\nu^3c^{-2}/(e^{h\nu/kT} - 1)$$
$$= 1.4745 \times 10^{-50}\nu^3/(e^{4.79922\times10^{-11}\nu/T} - 1) \quad W\,m^{-2}Hz^{-1}sr^{-1}$$

Notes:

This figure shows the spectral radiance of blackbodies for a range of temperatures.

An aluminized mirror has a reflectivity of about 96% and by Kirchoff's law the emissivity is 4%. Then the spectral radiance of an aluminized mirror at room temperature is approximated by $0.04\, B_\lambda(300K)$.

From the Wien wavelength displacement law, the maximum of the blackbody emission is

$$\lambda_{\max}(\mu m) = 2897.8/T(K)$$

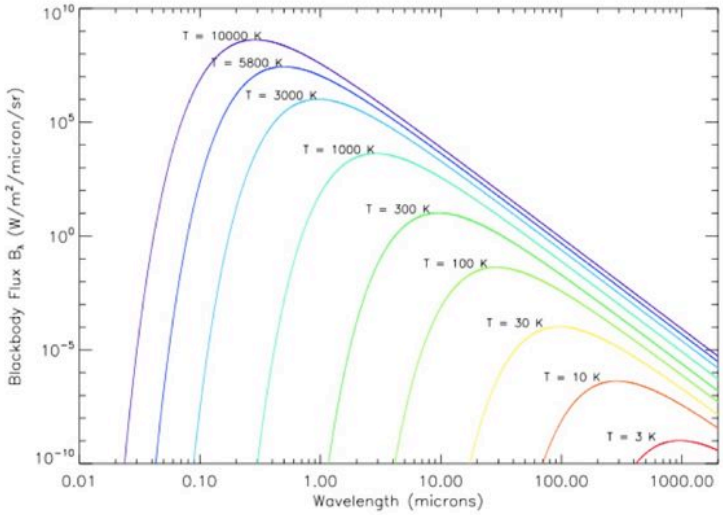

Notes:
From the Wien displacement law we can see that the maximum blackbody emission occurs near 10 μm for a room temperature object. Thus backgrounds are very high for mid-IR observations.

Conversion from F_λ to F_ν, where F_λ and F_ν are the flux density (spectral irradiance). The conversion equations are:

$$F_\lambda(W\ m^{-2}\mu m^{-1}) = \Omega B_\lambda,\quad F_\nu(W\ m^{-2}Hz^{-1}) = \Omega B_\nu,\quad F_\lambda = 3.0\times10^{14}F_\nu/\lambda_{\mu m}^2$$

where Ω is the solid angle in steradians.

Notes: